

Available online at [www.sciencedirect.com](http://www.sciencedirect.com)**ScienceDirect**

Procedia Engineering 99 (2015) 1158 – 1163

---

**Procedia  
Engineering**

---

[www.elsevier.com/locate/procedia](http://www.elsevier.com/locate/procedia)

“APISAT2014”, 2014 Asia-Pacific International Symposium on Aerospace Technology,  
APISAT2014

## Dimensional Measurement of Small Hot Pieces Based on a Monochrome CCD

Bi Chao<sup>a,b,\*</sup>, Qu Xinghua<sup>b</sup>, Liu Yong<sup>a</sup>, Liu Yaping<sup>a</sup>, Liu Jingliang<sup>a</sup>

<sup>a</sup>Aviation Key Laboratory of Science and Technology on Precision Manufacturing Technology, Beijing Precision Engineering Institute for Aircraft Industry, Beijing 100076, China

<sup>b</sup>State Key Laboratory of Precision Measuring Technology and Instrument, Tianjin University, Tianjin 300072, China

---

### Abstract

For the purpose of controlling the quality of forging process, a low-priced monochrome CCD is adopted to establish a vision measurement system to gauge the two-dimensional sizes of hot parts accurately in the paper. To derive the two dimensions of the forgings, comparison measurement method is employed. In the system, images are taken by the CCD through an infrared filter to filter out the strong light emitted from the forgings. And then average filtering and morphological filtering are used to reduce the effect of image noise. In order to improve the precision of geometry position, image distortion is corrected to reduce the optical distortion errors. After that, the edges in images are extracted at sub-pixel level to improve the location accuracy of geometry features. After calibration, the horizontal equivalent size of a pixel is 0.119mm, while the vertical 0.120mm. As be verified, the horizontal measurement uncertainty is 0.0069mm, while vertical 0.0063mm. Images of a 45<sup>#</sup> steel cuboid at 1000°C are captured and its dimensions are calculated through the procedure described in the paper, which have a difference less than 0.5mm compared with the theoretical values, indicating the precision and practicality of the method proposed in the paper.

© 2015 The Authors. Published by Elsevier Ltd. This is an open access article under the CC BY-NC-ND license

(<http://creativecommons.org/licenses/by-nc-nd/4.0/>).

Peer-review under responsibility of Chinese Society of Aeronautics and Astronautics (CSAA)

**Keywords:** Hot parts; Machine vision; Sub-pixel; Least squares fitting

---

---

\* Corresponding author. Tel.: +86-010-68380521-4130; fax: +86-010-68380416.

E-mail address: [773721278@qq.com](mailto:773721278@qq.com)

This research was supported by the Technology Innovation Found of AVIC (Grant No. 2011F30324).

## 1. Introduction

In the field of aeronautical manufacturing, forgings are always used as blanks of so many key parts of aircrafts due to their excellent performance. For the purpose of controlling the quality of forging process, on-line dimensional measurement of their size is always necessary. Considering the drawbacks of manual measurement with simple apparatus, non-contact measuring methods with industrial cameras has become the research focus of dimensional measurement of high-temperature forgings.

As the automation technology develops, vision measurement and detection methods are used in industrial field widely. Ma Junfu *et al* built a computer vision system to study the method to improve the precision of forging size detection [1]. Dominik Sankowski *et al* established a “THERMO-WET” system to measure the surface tension of molten metal using vision measurement technology [2].

As to many small forging products in aviation field, the blanks of them are always forged to certain shapes and then executed the next process. In the paper, a low cost monochrome CCD and an infrared filter are adopted to establish a vision measurement system to gauge the two-dimensional sizes of small hot ones accurately. Based on the spectral radiation characteristics of workpieces at high temperature, physical filtering is used to decrease the strong light from the hot ones; and then distortion correction, noise suppression and calibration of equivalent size of a pixel *etc* is executed. Several standard gauging blocks are utilized to verify the calibration results and test the measuring uncertainty of the system. Finally, a cuboid made of 45# steel is measured by the system, which shows good practicality and high precision of the system.

## 2. Measurement principle based on CCD

A digital image is composed of so many pixels, whose real dimension is uncertain that the same pixel in different images represents different sizes (*i.e.* the equivalent size of a pixel)[3]. To derive the real size of a target, the corresponding relationship between the pixel and its real size must be established. As a result, several standard gauging blocks are employed to calibrate the equivalent size of the pixel in the system environment.

After the working distance of the system is determined, the standard gauging block with nominal size  $L_0$  is placed at the working distance and then captured by the CCD through its optical system. After that, the number of pixels  $N$  between the two edges corresponding to the two measurement planes of the gauging block is acquired by image processing to calculate the equivalent size of a pixel represented by  $K$ , as can be expressed as follows:

$$K=L_0/N \quad (1)$$

Without changing anything, when the system is used to measure a target with unknown dimensions, it needs to place the target at the position of the gauging block mentioned above. Afterwards, the number of pixels  $N'$  along the direction of dimension to be measured can be used to compute the size of the target represented by  $L$ .

$$L=K \cdot N' \quad (2)$$

Strictly speaking, the shape of a pixel is not square, so its length and height are not the same. Therefore, gauging blocks being placed horizontally and vertically are captured to calibrate the equivalent sizes of a pixel in horizontal and vertical direction respectively. Due to the errors brought by calibration procedure, average of several measuring results is utilized to calculate the parameter  $K$ .

## 3. Components of the system

A cuboid made of 45# steel with the dimension of 30\*30\*40mm<sup>3</sup> is used as the experiment material, whose initial forging temperature is 1200℃ while final 800℃. Consequently a box-type resistance furnace is adopted as heating equipment, whose heating element is silicon carbide rods, power rating is 4kW and maximum heating temperature is 1300℃. Also, the furnace is equipped with a temperature-controlled cabinet, whose precision is  $\pm 1^\circ\text{C}$ .

As to imaging device, an integral monochrome camera CS8620Ci from Toshiba Corporation of Japan is selected, whose dimension of CCD is 1/2 inch, resolution is 752\*582 and signal-to-noise ratio is 60dB. Moreover, a manual iris lens from Pentax Corporation of Japan is chosen to work in conjunction with the camera, whose fixed focal length is 35mm and maximum aperture is F2.8. For the sake of protecting the camera from the heat of the forging and furnace, the camera is placed in a plastic box with two fans.

In order to improve the quality of images of high temperature parts, an infrared filter from Edmund Optics is employed to install in front of the lens to filter out the interference spectrum emitted from the hot parts. So that the images will be more distinct and the accuracy of image processing will be improved.

#### 4. Algorithm of image processing

##### 4.1. Physical filtering

According to the Planck Blackbody Radiation Formula, the radiation spectrum of hot parts between 800°C and 1200°C is principally strong red light and infrared light whose wave length is longer than 600nm. In practical measuring scene, physical filtering technology can be used to attenuate the disturbance of strong light.

Physical filtering can be achieved by using optical filters. The filters installed in front of lens can control the light which enters the lens. Through selection, the wave band needed can enter the lens while others absorbed. In the process of imaging hot parts, high temperature radiation and halation around the hot pieces can make the image quality decrease largely. Therefore, an infrared filter is installed in front the lens to attenuate the strong light in infrared band to derive high quality images.

##### 4.2. Distortion correction

Image distortion can be caused by the error of manufacture and installation of the imaging system, also the abnormality of photosensitive pixels. Thus image distortion has a bad influence on the accuracy of imaging geometry and position, which can bring in large computing errors to measuring results of the target [4].

For the purpose of improving the precision of distortion correction, an infrared filter is installed in front of the lens to make up the imaging unit as a whole, and then the Zhang Zhengyou's method is adopted. In the procedure of distortion correction, it needs to capture several images of the correction board from different angles using the CCD, in which the CCD can move arbitrarily and its special position need not to be known. A chessboard with 12\*12 squares whose size is 5mm\*5mm is used as correction board. It is pasted to a flat board after printed by the HP laser printer HPCP6015. In the paper, 20 images of the chessboard are captured by the CCD at different position and attitude to execute distortion correction. And one of the images of the chessboard is presented in *Fig.1 (a)*.

##### 4.3. Image Denoising

In the procedure of capturing pictures with CCD, the noise cannot be avoided, which can bring in errors to vision measurement results [6, 7]. As a result, it needs to calibrate the characteristics of the noise of CCD. Generally speaking, the noise can be divided as dark current noise and random noise.

The dark current noise shows the output of CCD when there is no light arriving at the photosensitive pixels. To reduce its influence on images, 20 images are captured when the aperture is closed and the average of them is used as the evaluation image of the dark current noise. And then the dark current noise can be restrained when every image subtracts this evaluation image. As to random noise, median filtering and mathematical morphology filtering methods are used to reduce the random noise and sustain the distinct edges at the same time.

##### 4.4. Sub-pixel edges detection

In image processing, detection and location of edges is very important. The precision of operators such as Sobel, Canny and LOG *etc* is always at integral pixel level. As application of machine vision technology deepens in the

industry field, the request of accuracy improves, which cannot be satisfied by location at integral pixel level. If improvement of the resolution of vision system is the only way used to deal with the problem, it is always uneconomic, sometimes even unpractical.

For the purpose of improving the position precision, edge location method at sub-pixel level based on least squares fitting is utilized in the paper. At first, Sobel operator is used to locate the edges initially to determine the position of the edges at integral pixel level. And then the pixels on the edge are extracted to execute least squares fitting to derive the edge position at sub-pixel level. Once the mathematic model is certain, the primary problem is the evaluation of the parameters. On the edge,  $n$  discrete pixels  $(x_i, y_i)(i=1,2,3,\dots,n)$  are extracted to fit the line expressed as  $y=ax+b$  by least squares method. Take

$$E(a,b)=\sum_{i=1}^n(y_i-a \cdot x_i-b)^2 \quad (3)$$

as the sum of squared residuals. If the minimum of  $E(a, b)$  is needed, the first order partial derivative of it to  $a$  and  $b$  must be equal to 0. So, the least squares evaluation of  $a$  and  $b$  can be derived as

$$\begin{cases} \frac{\partial E(a,b)}{\partial a} = -2 \cdot \sum_{i=1}^n (y_i - a \cdot x_i - b) \cdot x_i = 0 \\ \frac{\partial E(a,b)}{\partial b} = -2 \cdot \sum_{i=1}^n (y_i - a \cdot x_i - b) = 0 \end{cases}, \quad i=1,2,\dots,n \quad (4)$$

After the least squares line  $y=ax+b$  of one edge in the gauging block image is derived,  $m$  discrete pixels  $(x_j, y_j)(j=1,2,3,\dots,m)$  of the other edge are extracted. The distances between these pixels and the fitting line can be computed by Eqn.5. The average of them is used as the distance expressed by pixels between the two edges, which is known as  $N$  in Eqn.1.

$$d_j = \frac{|a \cdot x_j - y_j + b|}{\sqrt{a^2 + 1}}, \quad j=1,2,\dots,m \quad (5)$$

## 5. Experimentation and Results

### 5.1. Calibration of the equivalent size of a pixel

The working distance is set to 50cm after the experiment platform is set up, as shown in Fig.1 (b). Several standard gauging blocks are selected to calibrate the equivalent size of a pixel in the image. The blocks whose normal dimension are 10mm, 30mm and 50mm are used to calibrate the horizontal equivalent size of a pixel when they are placed horizontally, while to calibrate vertical one when placed vertically. Ten images of every block are captured by the system to calculate the parameter  $K$ , whose average is used as the final calibration result.

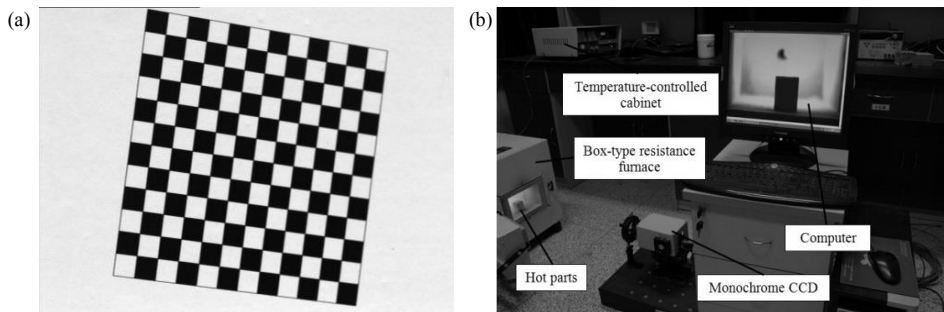


Fig.1. (a) One of the images of the chessboard; (b) Scene of experiments

The distance expressed by pixels between the two edges and their accurate position can be derived through the method described in Section 4.4. After that, calculation of the equivalent size of a pixel  $K$  can be executed through Eqn.1, and the results can be seen in Table.1.

Table 1. Calibration results of the equivalent size of a pixel

| Nominal size<br>/mm | Distance expressed by<br>pixels/pixel |            | Equivalent size of a<br>pixel/(mm/pixel) |            | Average/(mm/pixel) |            |
|---------------------|---------------------------------------|------------|--|------------|--------------------|------------|
|                     | Horizontally                          | Vertically | Horizontally                             | Vertically | Horizontally       | Vertically |
| 10                  | 83.93                                 | 82.67      | 0.1191                                   | 0.1210     |                    |            |
| 30                  | 252.18                                | 250.56     | 0.1190                                   | 0.1197     | 0.11893            | 0.12007    |
| 50                  | 421.30                                | 418.47     | 0.1187                                   | 0.1195     |                    |            |

In Table.1, the column “Average” expresses the average of equivalent size of a pixel of these blocks being placed horizontally and vertically respectively, which is used as the final calibration result. As can be seen, the difference between the equivalent size of a pixel in horizontal direction and that in vertical direction is so tiny that the results can meet the practical requests.

5.2. Verification of calibration results

In order to verify the calibration results and derive the measuring uncertainty of the system, another standard blocks of 9mm, 20mm, 40mm and 60mm are used to test the system. Firstly, every block is placed horizontally to take 20 images and then distortion correction, noise depression and sub-pixel edge detection is executed to compute the size of the block in the image through Eqn.2. And the average is used as the final result. Secondly, they are placed vertically to compute the results through the same procedure. Table.2 shows the results of the 4 kinds of gauging blocks mentioned above.

Table.2 Measuring results of the 4 kinds of gauging blocks

| Direction    | Nominal size/mm | Distance expressed by<br>pixels/pixel | Measuring results/mm | Absolute error/mm | Relative error/% | Standard deviation/mm | Average of standard deviation/mm |
|--------------|-----------------|---------------------------------------|----------------------|-------------------|------------------|-----------------------|----------------------------------|
| Horizontally | 9               | 75.77                                 | 9.0110               | 0.0110            | 0.1222           | 0.0019                | 0.0023                           |
|              | 20              | 168.19                                | 20.0033              | 0.0033            | 0.0165           | 0.0023                |                                  |
|              | 40              | 336.87                                | 40.0636              | 0.0636            | 0.1590           | 0.0032                |                                  |
|              | 60              | 505.47                                | 60.1181              | 0.1181            | 0.1968           | 0.0018                |                                  |
| Vertically   | 9               | 75.28                                 | 9.0389               | 0.0389            | 0.4322           | 0.0011                | 0.0021                           |
|              | 20              | 166.97                                | 20.0477              | 0.0477            | 0.2385           | 0.0022                |                                  |
|              | 40              | 334.37                                | 40.1475              | 0.1475            | 0.3687           | 0.0015                |                                  |
|              | 60              | 502.06                                | 60.2823              | 0.2823            | 0.4705           | 0.0034                |                                  |

As can be seen in Table.2, the horizontal standard deviation of the system is 0.0023mm, while vertical 0.0021mm. According to the error theory, the measuring uncertainty is three times the standard deviation. Thus the horizontal measuring uncertainty of the system is 0.0069mm, while the vertical 0.0063mm, which can meet the practical requests.

### 5.3. Results of Experiments

Before the workpiece is heated, a fifty indexing calliper is used to measure the length and width of it 10 times respectively, and the average is used as the size of it at normal temperature. After measuring, the length and width of the part are 39.12mm and 28.74mm respectively. The theoretical size of it  $L$  at 1000°C can be calculated through Eqn.6.

$$L=L_0 \cdot [1+\lambda \cdot (T-T_0)] \quad (6)$$

In which  $T$  represents the temperature of the hot part,  $T_0$  the normal temperature; and  $L_0$  is the dimension of it at the temperature of  $T_0$ , while  $L$  at  $T$ . The parameter  $\lambda$  represents the linear thermal expansion coefficient of the material. In the paper, the 45# steel will be measurement at 1000°C, so  $\lambda$  is equal to  $15.08 \times 10^{-6}/^\circ\text{C}$ . Finally, the theoretical values of the length and width of the hot part are 39.710mm and 29.173mm respectively.

The cuboid made of 45# steel is placed in the furnace and adjusted to the position of the working distance, which will be heated to 1000°C. Ten images of the forging are taken through the system. The measuring results after the procedure mentioned in the paper can be seen in Fig.2 (a) and Fig.2 (b). Through calculation, the length of the workpiece is 39.375mm, which has a difference of 0.335mm compared with the theoretical value; while the width 29.476mm, which has a difference of 0.303mm.

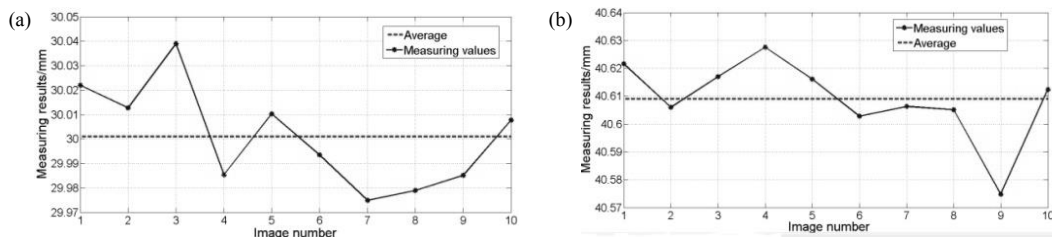


Fig.2. Measuring results of the hot part: (a) Width; (b) Length

## 6. Conclusion

A monochrome CCD and infrared filter *etc* are used to establish a machine vision system to execute precise measurement of two dimensional sizes of hot parts in the paper. Based on the radiation characteristics of high temperature forgings, physical filtering technology is used to decrease the interference of strong light to improve the image quality. And then, distortion correction, noise depression and calibration of equivalent size of a pixel *etc* are executed. In order to verify the calibration results, several standard gauging blocks are selected to test the system, which shows the measuring uncertainty is 0.0069mm in horizontal direction while 0.0063mm in vertical. Finally, the system is used to measure a hot part and its dimensions are computed, which is smaller than 0.5mm compared with the theoretical values. So the good practicability and high accuracy of the system is shown.

## References

- [1]J.F. Ma, X.J. Zhou, Z.N. Xu, J. Chi, Study on the Edge Detection of Forging Based on Computer Vision, Modular Machine Tool & Automatic Manufacturing Technique. 11 (2007) 48-50.
- [2]A. Fabijanska, D. Sankowski, Computer vision system for high temperature measurements of surface properties, Machine Vision and Applications. 20 (2009) 411-421.
- [3]J.T. Yuan, L. Yang, X.C. Wang, J. Zhang, R.X. Jin, Measurement and Analysis of Water Mist Droplet Size Based on Machine Vision, Acta Optica Sinica. 29. 10(2009) 2842-2847.
- [4]C.Z. Su, E. G. Wang, J.T. Hao, G.H. Cao, H.J. Xu, Distortion correction for images in planar metrology, Optics and Precision Engineering. 19. 1(2011) 161-167.
- [5]J.Y. Zhang, Flexible Camera Calibration by Viewing a Plane from Unknown Orientations, The Proceedings of the Seventh IEEE International Conference on Computer Vision, Kerkyra, Greece. 1 (1999) 666-673.
- [6]X.H. Ding, Y. Li, Q.F. Yu, W.D. Feng, CCD Noise Calibration and its Application in Edge Location, Acta Optica Sinica. 28. 1 (2008) 99-104.
- [7]X.Z. Xu, Z.T. Li, L.J. Xue, Analysis and processing of CCD noise, Infrared and Laser Engineering. 33.4 (2004) 343-357.